Angle-of-Attack Control of Spinning Missiles

D. H. Platus*
The Aerospace Corporation, El Segundo, Calif.

The application of controlled wind-fixed pitch and yaw moments to control the coning angle of a spinning missile is described. The open-loop response to applied pitch and yaw moments is derived, and the closed-loop behavior of an angle-of-attack control system is analyzed. The angle-of-attack undamping due to a yaw moment is shown to be equal to that for steady roll resonance, and resonance is shown to be a limiting case of yaw moment undamping when the roll rate is equal to the critical frequency. The practical implementation of an angle-of-attack control system is described, and several applications are discussed including passive angle-of-attack damping, roll lockin prevention, and drag control.

Nomenclature

A_D = drag acceleration
A_L = lift acceleration
A_R = resultant of lift and drag accelerations
A_x = axial acceleration
A_{z_w} = normal acceleration in lift plane
C_{m_q} = aerodynamic pitch or yaw damping derivative
C_{N_α} = aerodynamic normal force derivative
d = aerodynamic reference diameter
I = pitch or yaw moment of inertia
I_x = roll moment of inertia
j = $(-1)^{1/2}$
k = pitch or yaw radius of gyration, $(I/m)^{1/2}$
K = control system gain, $K_1K_2M_p/I$
m = missile mass
M = body-fixed trim moment
M_p = wind-referenced pitch moment
M_y = wind-referenced yaw moment
p = roll rate
p_1,p_2,p_3 = closed-loop roots
q = wind-referenced pitch rate, $\dot{\theta}$
q_∞ = dynamic pressure
r = wind-referenced yaw rate, $\dot{\psi}\sin\theta$
s = Laplace transform variable, $\sigma+j\omega$
S = aerodynamic reference area
t = time
u = missile velocity
x_{st} = static margin (distance of center of pressure aft of center of mass)
γ = angle between missile axis and A_R
δ = equivalent control deflection
ζ = pitch or yaw damping ratio,

$$\frac{1}{2m}\left(\frac{\rho SI}{2C_{N_\alpha}x_{st}}\right)^{1/2}(C_N-C_{m_q}d^2/2k^2)$$

θ = coning half angle (Euler angle)
θ_c = angle-of-attack command
θ_t = nonrolling, body-fixed trim angle of attack, M/ω_n^2I
$\dot{\theta}$ = wind-referenced pitch rate
λ = ratio of roll rate to critical frequency, $p/\pm\omega_n$
ρ = atmospheric density
σ = real part of s
ϕ = roll angle relative to wind (Euler angle)
$\dot{\phi}$ = windward meridian rotation rate
$\dot{\phi}_{+,-}$ = body frequencies
ψ = precession angle (Euler angle)
$\dot{\psi}$ = precession rate
$\dot{\psi}_{+,-}$ = precession modes
ω = imaginary part of s
ω_n = natural pitch frequency, $(C_{N_\alpha}q_\infty Sx_{st}/I)^{1/2}$
Ω = body frequency, $\dot{\phi}_{+,-}$

Superscript

( ) = differentiation with respect to time

Presented as Paper 74-821 at the AIAA Mechanics and Control of Flight Conference, Anaheim, California, August 5-9, 1974; submitted August 13, 1974; revision received November 18, 1974. This work was supported by the U.S. Air Force under Contract F04701-73-C-0074.

Index categories: Entry Vehicle Dynamics and Control; LV/M Dynamics and Control; Entry Deceleration Systems and Flight Mechanics.

*Staff Scientist. Member AIAA.

I. Introduction

It is well known that a yaw or side moment produced by a force that acts perpendicular to the pitch plane of total angle of attack can produce a Magnus-type dynamic instability. The classical Magnus moment is proportional to the spin rate and angle of attack of the spinning missile, and Magnus type effects on stability have been investigated extensively.[1-8] Yaw moment instabilities produced by other phenomena have also been demonstrated.[9-12] A characteristic of Magnus-type angle-of-attack undamping is almost purely circular coning motion.[3,10] As the angle of attack undamps, the character of the motion changes markedly from the trimmed lunar motion condition, where the precession rate is approximately equal to the roll rate, to a rotary windward meridian condition, where the precession rate is approximately equal to the pitch frequency.[10,13] These characteristics indicate that 1) the angle of attack might be controlled by imposing a controlled side force or yaw moment, 2) the resulting drag should be predictable from the nearly constant angle of attack in circular motion, and 3) the induced precession and windward meridian rotation rates might be used advantageously, e.g., to prevent roll lockin during resonance crossing.

II. Analysis

A. Open-Loop Response to Wind-Fixed Moments

It is convenient to describe the rotational motion in terms of the classical Euler angle coordinates defined in Fig. 1. The moment equations of motion for a slowly rolling, axisymmetric missile subjected to wind-fixed pitch and yaw moments M_p and M_y, respectively, and a body-fixed trim moment M can be written approximately (for small θ and $I_xp/2I \ll \omega_n$)[13,14]

$$\ddot{\theta}+2\zeta\omega_n\dot{\theta}+(\omega_n^2-\dot{\psi}^2)\theta=M_p/I+(M/I)\cos\phi \qquad (1)$$

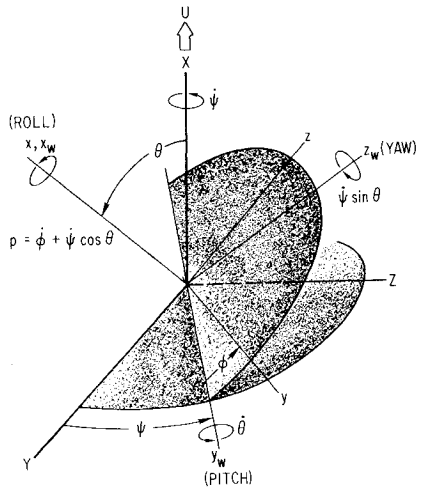

Fig. 1 Euler angle coordinates. X, Y, Z = inertial coordinates; x, y, z = body-fixed coordinates; x_w, Y_w, z_w = wind-referenced coordinates ψ, ϕ, θ = Euler angles.

$$2\dot\psi\dot\theta + (\ddot\psi + 2\zeta\omega_n\dot\psi)\theta = M_y/I + (M/I)\sin\phi \tag{2}$$

$$p = \dot\phi + \dot\psi \tag{3}$$

where ω_n is the natural pitch frequency, and ζ is the aerodynamic pitch or yaw damping expressed as a critical damping ratio, (see Nomenclature). If we consider the response to the wind-fixed moments when $M = 0$, we find that a condition for steady coning motion ($\dot\theta = \ddot\theta = \ddot\psi = 0$) is

$$\dot\psi_{+,-} = \omega_n\{-\zeta M_p/M_y \pm [1 + (\zeta M_p/M_y)^2]^{1/2}\} \tag{4}$$

which is approximately $\dot\psi_{+,-} = \pm\omega_n$ for $\zeta M_p/M_y \ll 1$. The quasi-steady response to the applied moments is obtained by solving Eq. (2) for θ with $\ddot\psi = 0$ and $\dot\psi = \dot\psi_{+,-}$, which yields, for the coning half angle,

$$\theta(t) = \frac{M_y}{2\zeta\omega_n I\dot\psi_{+,-}}(1 - e^{-\zeta\omega_n t}) + \theta(0)e^{-\zeta\omega_n t} \tag{5}$$

where the precession mode corresponds with the sign of M_y (Fig. 2), i.e., a positive yaw moment induces positive precession, and a negative yaw moment induces negative precession. The corresponding windward meridian rotation rate from Eq. (3) is $\dot\phi_{+,-} = p - \dot\psi_{+,-}$ (Fig. 2), which is of opposite sign to $\dot\psi_{+,-}$ for subcritical roll rates $|p| < \omega_n$. Thus, a wind-fixed yaw moment induces an undamping of the angle of attack† that reaches a steady-state value $M_y/2\zeta\omega_n^2 I$, which is precisely the steady resonance amplification of a nonrolling trim angle of attack $M_y/\omega_n^2 I$ that would be produced if M_y were body fixed. However, Eq. (5) applies independent of roll rate. The steady resonance condition is obtained readily from Eqs. (1-3) with $M_p = M_y = 0$. In steady trimmed motion, the windward meridian rotation rate $\dot\theta$ is zero, the precession rate $\dot\psi$, from Eq. (3), is approximately equal to the roll rate, and a steady coning condition $\dot\theta = \ddot\theta = \ddot\psi = 0$ exists for

$$\phi = \tan^{-1}[2\zeta\lambda/(1 - \lambda^2)] \tag{6}$$

$$\theta = \frac{\theta_t}{[(1 - \lambda^2)^2 + (2\zeta\lambda)^2]^{1/2}} \tag{7}$$

†In steady coning motion, the total angle of attack differs from the coning half angle by an increment of order $\omega_n k^2\theta/ux_{st}$ because of lateral translation of the center of mass, which is negligible for most purposes. Angle of attack and coning half angle are hereafter used interchangeably.

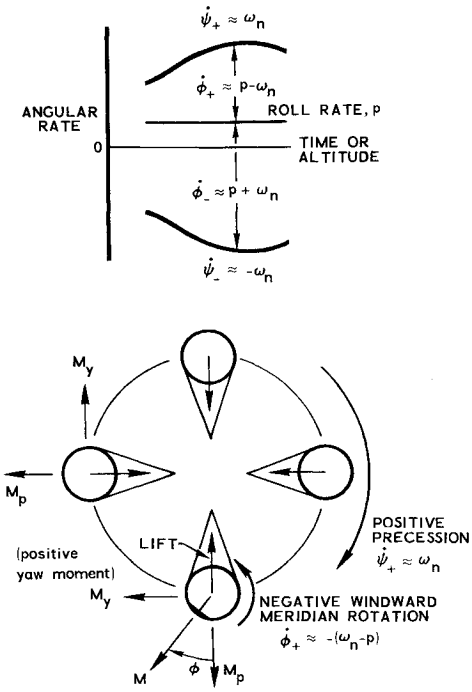

Fig. 2 Yaw moment-induced coning motion.

where $\lambda \equiv p/\pm\omega_n$, and $\theta_t \equiv M/\omega_n^2 I$ is the nonrolling trim angle of attack produced by the body-fixed moment M. These familiar expressions have been derived previously.[15,16] As the roll rate approaches resonance, $\lambda \to 1$, $\phi \to 90°$ and the body-fixed trim moment becomes a yaw moment (Fig. 2). The steady resonance amplification from Eq. (7) is, then, $\theta = \theta_t/2\zeta = M/2\zeta\omega_n^2 I$, which, from Eq. (5), is the steady angle-of-attack response to a yaw moment as $t \to \infty$. Since Eq. (5) is applicable independent of the roll rate ratio λ or windward meridian rotation rate $\dot\phi$, the trim angle-of-attack amplification during steady resonance is a special case of the response to a yaw moment when $p = \omega_n$, for which the two conditions coincide. A striking feature of yaw-moment-induced undamping is the induced precession of the lift vector at the pitch frequency and corresponding windward meridian rotation rate. This is in contrast to the lunar motion trimmed condition, where the windward meridian rotation rate is zero, and the lift vector precesses at the roll rate. Yaw undamping can even occur at zero roll rate for which $\dot\psi = -\dot\phi = \pm\omega_n$. An example of this is shown later.

B. Closed-Loop Angle-of-Attack Control

Let us assume that an arbitrary wind-fixed moment with components M_p and M_y can be generated for control purposes and define δ as the equivalent "control deflection" or the fraction of full-scale moment generated. If we perturb Eqs. (1) and (2) in θ and $\dot\psi$ about the quasi-steady values $\theta = \bar\theta$ and $\dot\psi = \omega_n$ and neglect damping and all but first-order terms in the perturbed quantities, the resulting linearized control equations after Laplace transformation can be written

$$\begin{bmatrix} s^2 & -2\omega_n\bar\theta \\ 2\omega_n s & s\bar\theta \end{bmatrix} \begin{bmatrix} \theta(s) \\ \dot\psi(s) \end{bmatrix} = \begin{bmatrix} M_p/I \\ M_y/I \end{bmatrix}[\delta] + \begin{bmatrix} \dfrac{s}{s^2 + \Omega^2} \\ \dfrac{\Omega}{s^2 + \Omega^2} \end{bmatrix}[M/I] \tag{8}$$

where $\theta(s)$ and $\dot{\psi}(s)$ are now the perturbations about $\bar{\theta}$ and ω_n, respectively, Ω is the windward meridian rotation frequency $p-\omega_n$, and s is the Laplace transform variable.‡ We assume a control law of the form

$$\delta = K_1[\theta_c(s) - \theta(s) - K_2 s\theta(s)] \tag{9}$$

which corresponds to the block diagram of Fig. 3, where θ_c is the input command value of the angle of attack and θ is the closed-loop response. If we consider only the response to the control moment, the open-loop transfer function $G(s)\,H(s)$ of the closed-loop characteristic equation $1+G(s)\,H(s)=0$ is, from Eqs. (8) and (9),

$$G(s)H(s) = \frac{K(s+1/K_2)(s+2\omega_n M_y/M_p)}{s(s^2+4\omega_n^2)} \tag{10}$$

where $K=K_1K_2M_p/I$. The root locus of the characteristic equation is shown in Fig. 4. Because the departure angle from the imaginary poles is $\psi_1+\psi_2$, the system will be stable for all values of gain for $\psi_1+\psi_2 \geq \pi/2$. Numerical values of the root locus are shown for $\psi_1=\psi_2=\pi/4$ with $\omega_n=50$ rad/sec, which corresponds to $M_p=M_y$ and $K_2=1/2\omega_n=0.01$. The system shows good stability characteristics and is relatively insensitive to the ratio M_y/M_p, which determines the orientation of the control moment relative to the wind.

The closed-loop response to the body-fixed trim moment is obtained by substituting for δ from Eq. (9) in Eq. (8), with $\theta_c=0$, which yields

$$\begin{bmatrix} s^2+K(s+1/K_2) & -2\omega_n\bar{\theta} \\ 2\omega_n s+K(M_y/M_p)(s+1/K_2) & s\bar{\theta} \end{bmatrix} \begin{bmatrix} \theta(s) \\ \dot{\psi}(s) \end{bmatrix} = \begin{bmatrix} \dfrac{s}{s^2+\Omega^2} \\ \dfrac{\Omega}{s^2+\Omega^2} \end{bmatrix} \begin{bmatrix} \omega_n^2\theta_t \end{bmatrix} \tag{11}$$

where θ_t is the nonrolling trim due to the body-fixed moment M. The closed-loop angle-of-attack response to θ_t is, from Eq. (11),

$$\frac{\theta(s)}{\theta_t} = \frac{\omega_n^2(s^2+2\omega_n\Omega)}{(s^2+\Omega^2)(s+p_1)(s+p_2)(s+p_3)} \tag{12}$$

where p_1, p_2, and p_3 are the closed-loop roots obtained from Fig. 4 for a specified value of the gain K. The magnitude of the steady-state response ratio θ/θ_t is

$$\left|\frac{\theta}{\theta_t}\right| = \frac{\omega_n^3(3-\lambda)}{\mathcal{L}_1\mathcal{L}_2\mathcal{L}_3} \tag{13}$$

where the zeros and poles of Eq. (12) are shown in Fig. 5, and $\mathcal{L}_1\mathcal{L}_2$, and $\mathcal{L}_3$ are the vector lengths from the closed-loop roots p_1, p_2, and p_3 to $s=-\Omega=i\omega_n(1-\lambda)$. For values of K that give good stability characteristics, Eq. (13) indicates that the steady-state trim response is attenuated for $\lambda \ll 3$. As $K\to 0$, $\mathcal{L}_1\to\omega_n(1-\lambda)$, $\mathcal{L}_2\to\omega_n(1+\lambda)$, and $\mathcal{L}_3\to\omega_n(3-\lambda)$, which reduces Eq. (13) to the open-loop trim amplification factor $\theta/\theta_t=(1-\lambda^2)^{-1}$ as expected. If the yaw moment induces negative precession while the roll rate is positive (or vice versa), then λ is negative, and the response to the trim is obtained from Eq. (13) and Fig. 5, with the sign of λ changed accordingly. Consequently, the precession mode does have an influence on the response to a body-fixed trim, depending on the system gain.

‡Although the perturbations are taken about an initial condition of positive precession, the results are applicable to either mode, except for the slight shift in precession frequency from $\pm\omega_n$, Eq. (4), and a slight difference in the closed-loop response to a body-fixed moment, which is shown later.

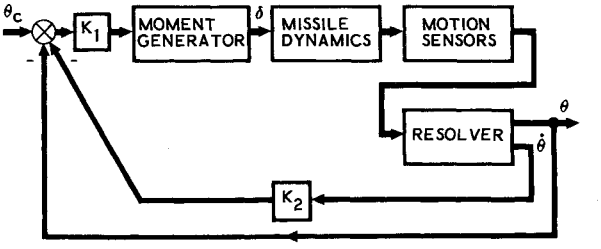

Fig. 3 Angle-of-attack control system block diagram.

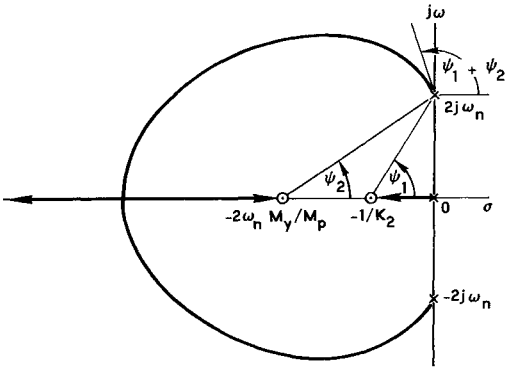

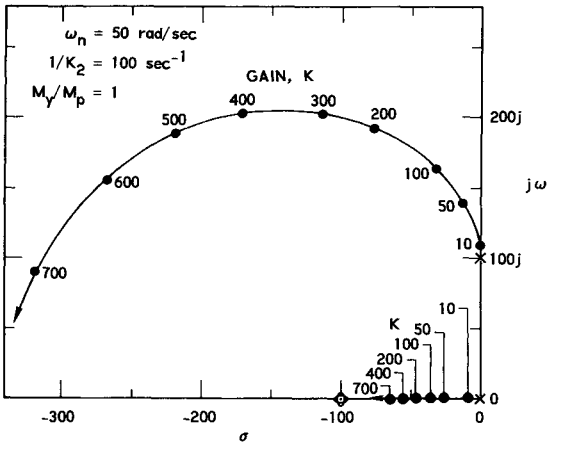

Fig. 4 Root locus for angle-of-attack control system.

The results of computer simulations of the closed-loop response of θ and $\dot{\psi}$ to step inputs in angle-of-attack command are given in Figs. 6 and 7, where the control parameters correspond to $K=100$ in Fig. 4. In both cases, the missile is initially trimmed because of a body-fixed moment that corresponds to 0.5° nonrolling trim, and a step input of 4° is applied at $t=0$. In Fig. 6, the roll rate (and initial precession rate $\dot{\psi}$) is zero, and a positive yaw moment is applied, which induces a positive precession $\dot{\psi}_+=+\omega_n$. In Fig. 7, the roll rate is initially at one-half the critical frequency, and a negative yaw moment is applied, which induces a negative precession rate. The moment equations of motion that were integrated numerically contain small additional roll rate terms that were not included in Eqs. (1) and (2) for simplicity,[13,14] but give the slightly more precise definition of precession frequencies

$$\dot{\psi}_{+,-} = I_x p/2I + [\omega_n^2 + (I_x p/2I)^2]^{1/2} \{-\zeta M_p/M_y \pm [1+(\zeta M_p/M_y)^2]^{1/2}\} \tag{14}$$

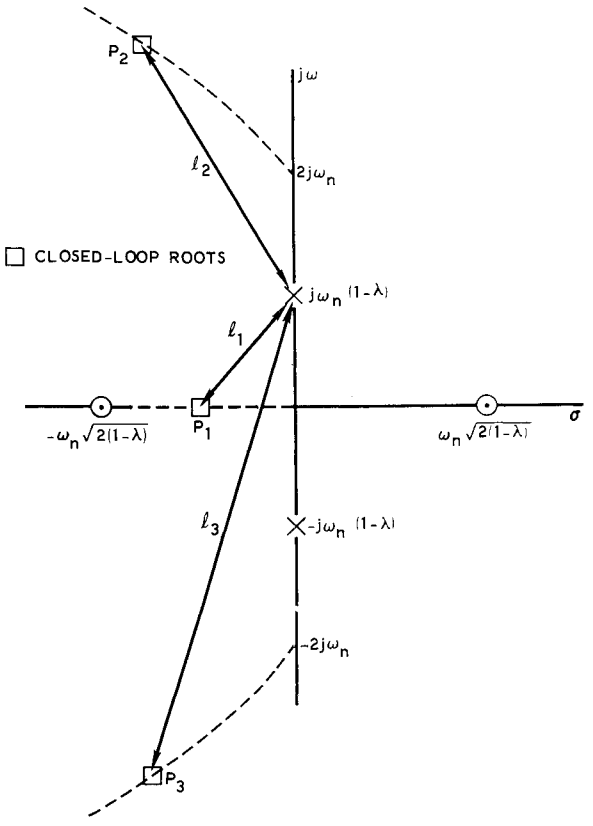

Fig. 5 Response to body-fixed trim.

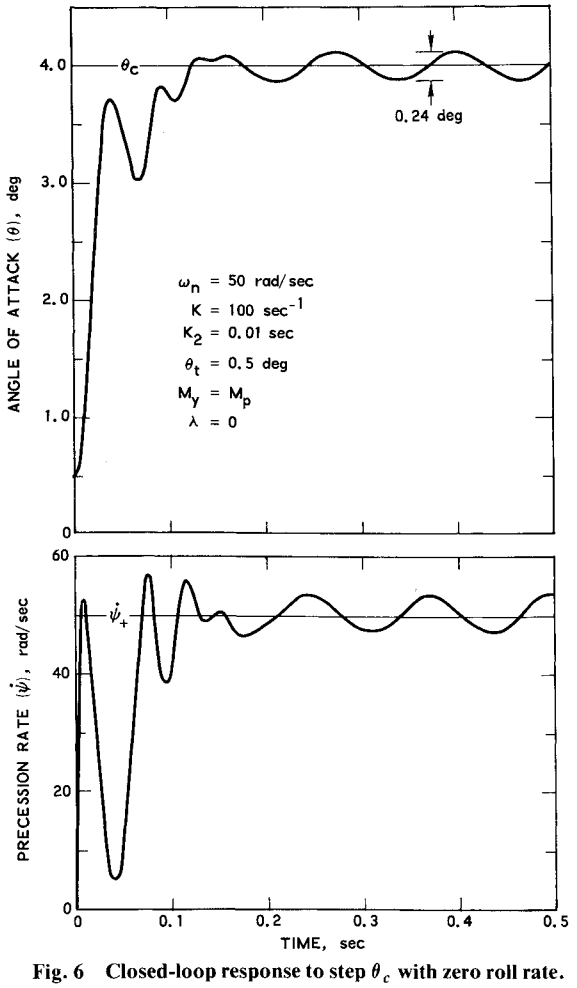

Fig. 6 Closed-loop response to step θ_c with zero roll rate.

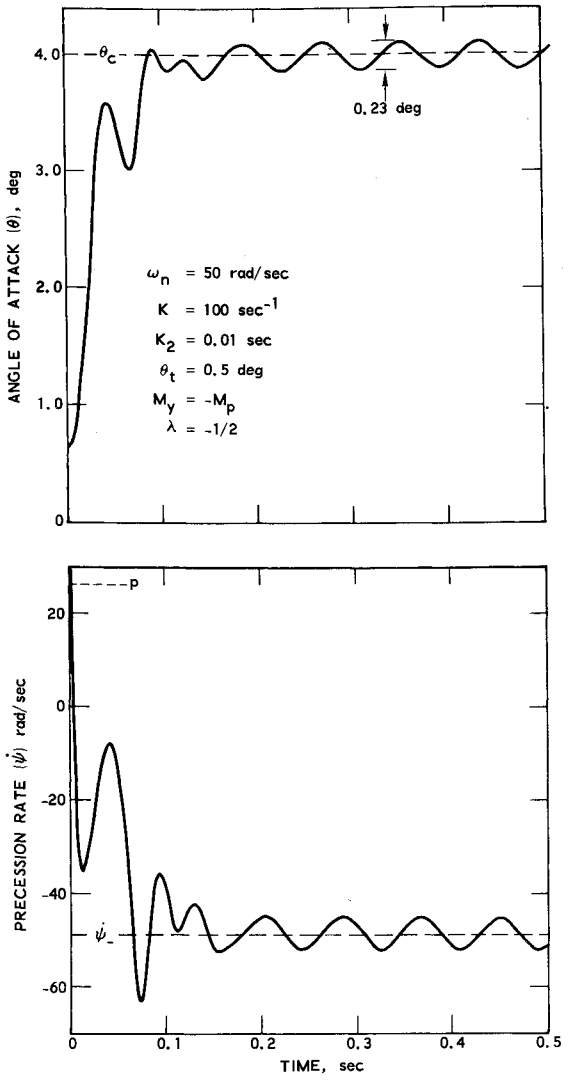

Fig. 7 Closed-loop response to step θ_c with roll rate at one-half the critical frequency.

compared with Eq. (4). With $\zeta=0$, as taken for the simulations, $\dot{\psi}_{+,-} \approx I_x p/2I \pm \omega_n$, which yields $\dot{\psi}_+ \approx 50$ rad/sec and $\dot{\psi}_- \approx -48.7$ rad/sec for the cases shown in Figs. 6 and 7, respectively.

The body-fixed trim results in an oscillation about θ_c that is attenuated in accordance with Eq. (13) and Fig. 5. For zero roll rate (Fig. 6), the 0.5° nonrolling trim is attenuated to 0.24 of its open-loop value, or 0.24° double-amplitude oscillation in contrast to a 1° oscillation that would exist open loop. Similarly, with the roll rate at one-half the critical frequency (Fig. 7), the 0.5° trim is amplified to 2/3 deg in the initial trimmed condition. The closed-loop response for this case yields an attenuation to 0.23 of the nonrolling trim value, or 0.23° double-amplitude oscillation, compared with a 1.33° oscillation that would exist open loop, i.e., the trim oscillation that would exist about any untrimmed value of θ.

While the foregoing analysis is based on the assumption of linear, small-angle aerodynamics, practical aerodynamic configurations often exhibit nonlinear pitch and yaw moments and yaw moment reversals. Angle-of-attack control applied to such systems would probably require slightly higher gain control systems to insure that the out-of-plane control moments always exceed the maximum anticipated aerodynamic yaw moments. For higher gain systems the closed-loop response would tend to be dominated by the linear control elements, which would minimize the effects of nonlinearities in the open-loop vehicle dynamics.

III. Control System Implementation

Implementation of the angle-of-attack control system requires a means of generating wind-fixed control moments and a sensor system for measurement of the pertinent motion response parameters. Because yaw moment undamping of the angle of attack produces, in general, a rotary windward meridian, the control force must rotate at one of the body frequencies and maintain a fixed orientation relative to the wind vector or lift plane. This can be accomplished in several ways by using a pendulum mass that aligns itself with the lift vector (Fig. 8). Any form of trim generator can be either passively stabilized by means of the pendulum mass or it can be motor driven at the windward meridian rotation frequency by using the pendulum to regulate the motor speed at the proper frequency. The desired ratio of pitch to yaw moment is obtained by orienting the trim generator at the proper angle relative to the lift vector.

A pendulum can also be used to orient a sensor system relative to the wind for direct measurement of the motion parameters in the Euler angle (wind-referenced) coordinate system. Such a sensor system is shown in Fig. 9. In addition to conventional body-fixed axial acceleration and roll rate sensors, pitch and yaw angular rate sensors and a normal acceleration sensor are mounted to a pendulum that rotates relative to the vehicle at the windward meridian rotation rate $\dot{\phi}$, which is measured directly. The pendulum mounted rate sensors measure pitch rate $q=\dot{\theta}$ and yaw rate $r=\dot{\psi}\sin\theta$ in the Euler angle system. From the definition of roll rate $p=\dot{\phi}+\dot{\psi}\cos\theta$, the angle of attack θ is obtained simply from the relation

$$\theta=\tan^{-1}\left(\frac{r}{p-\dot{\phi}}\right) \tag{15}$$

where p, r, and $\dot{\phi}$ are measured directly. The normal acceleration A_{z_w} in the lift plane is measured directly from the pendulum-mounted accelerometer. If C_{N_α} is known with sufficient accuracy, then A_{z_w} gives a direct measurement of θ. The resultant acceleration A_R and its orientation angle γ with respect to the missile axis are obtained from a resolution of A_x and A_{z_w} according to

$$A_R=(A_x^2+A_{z_w}^2)^{1/2} \tag{16}$$

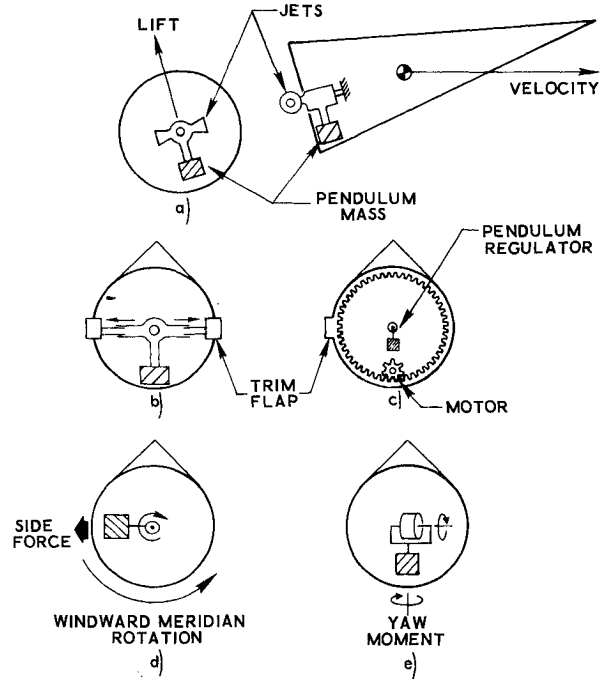

Fig. 8 Mechanization schemes. a) inertia-stabilized reaction jets; b) inertia-stabilized trim generator; c) motor-driven trim generator; d) motor-driven pendulum mass; e) inertia-stabilized gyro wheel.

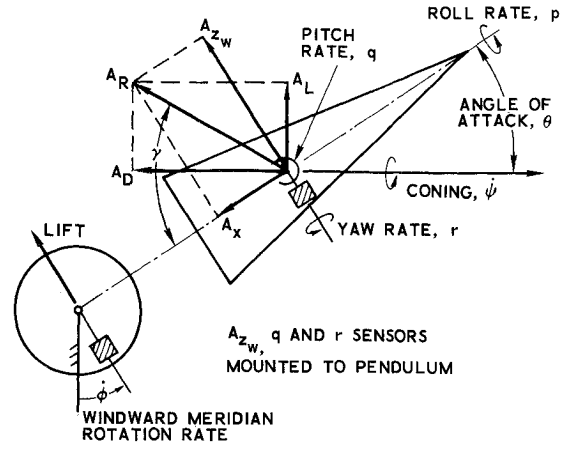

Fig. 9 Inertia-stabilized sensor system.

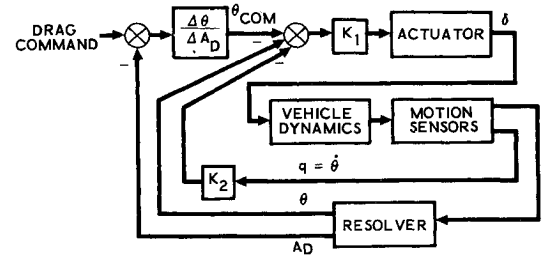

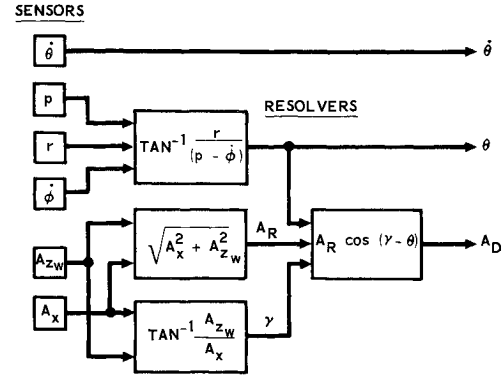

Fig. 10 Drag system control logic.

$$\gamma=\tan^{-1}(A_{z_w}/A_x) \tag{17}$$

The lift and drag acceleration are then obtained from the relations

$$A_L=A_R\sin(\gamma-\theta) \tag{18}$$

$$A_D=A_R\cos(\gamma-\theta) \tag{19}$$

The control logic for a drag control system in which drag is induced by angle of attack is shown in Fig. 10.

IV. Discussion

Potentially, angle-of-attack control can be used to damp the angle of attack, prevent roll lockin, or induce drag for deceleration or drag modulation. The undamping of angle of attack by a yaw moment has been described and is expressed analytically in Eq. (5). It has been demonstrated that either a positive or negative yaw moment will undamp the angle of attack and induce angular precession of the corresponding sign (Fig. 2). Conversely, if the angle of attack is undamped in either of the precession modes because of some extraneous

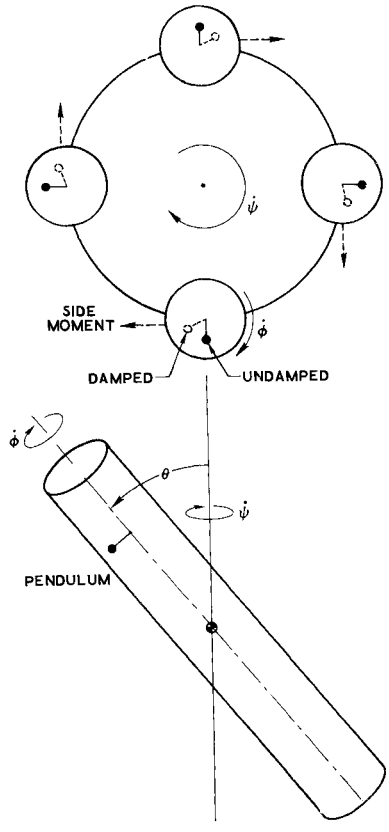

Fig. 11 Precession controller.

source, then an applied yaw moment in the opposite direction, one that opposes the precession, will damp that mode. The dominant precession mode can readily be sensed by the control system from a direct measurement of the windward meridian rotation rate $\dot{\phi}$. The average value of $\dot{\phi}$ is $p \mp \omega_n$, which corresponds to $\dot{\psi} = \pm\omega_n$. For example, for subcritical roll rates $|p| < \omega_n$, $\dot{\phi}$ will be either negative or positive, corresponding to positive or negative precession, respectively. Thus, the sign of the applied yaw moment to damp the angle of attack will correspond with the sign of $\dot{\phi}$.

An interesting possibility exists for a passive angle-of-attack damper. Hopper[17] has proposed a motor-driven pendulum mass to damp the precession angle (coning angle) of a spinning spacecraft and has shown that a passive damped pendulum would increase the coning angle. In the absence of external moments, the spin rate $\dot{\phi}$ and precession rate $\dot{\psi}$ are in the same direction and are related by $\dot{\phi} = (I/I_x - 1)\dot{\psi}\cos\theta$. If viewed along the coning axis, a pendulum mass displaced axially from the vehicle center of mass would align itself in the θ plane because of centrifugal force (Fig. 11). With viscous or friction damping resisting the pendulum rotation relative to the spacecraft, the pendulum would be displaced as shown in Fig. 11. In the displaced position, the pendulum mass exerts a side moment on the spacecraft analogous to a yaw moment on a spinning missile. Because this moment is in the direction that reinforces the precession, the coning angle will increase Hopper has proposed to actively drive the pendulum in the opposite direction to oppose the precession motion and thus damp the coning angle.

The rotational motion of a spinning missile subject to aerodynamic pitch and yaw moments is somewhat different from that of the moment-free spacecraft, as indicated by a comparison of Figs. 2 and 11. For subcritical roll rates, the spin rate $\dot{\phi}$ of the missile is in a direction opposite to the precession rate, as illustrated in Fig. 2. Consequently, the passive damped pendulum that induces an increase in coning angle of the moment-free spacecraft will damp the coning angle of a spinning statically stable missile with subcritical roll rate if located aft of the center of gravity. For supercritical roll rates, which characterize the high-altitude motion of a spinning reentry vehicle, the precession mode depends on the orientation of the exoatmospheric precession cone relative to the velocity vector.[13] The passive pendulum damper will damp negative precession and undamp positive precession because $\dot{\phi} \approx p - \omega_n$ is always positive, whereas $\dot{\psi} \approx \pm\omega_n$. If the exoatmospheric precession cone is damped out, e.g., by use of the active damper proposed for spacecraft, the re-entry vehicle will precess negatively provided that there is an initial angle-of-attack misalignment (angle between the velocity vector and the angular momentum vector of the initial precession cone).[13] The subsequent angle-of-attack convergence would then be accelerated by use of the aft-mounted passive damped pendulum.

Angle-of-attack control can be used to prevent resonance lockin by undamping the angle of attack at resonance crossing sufficiently to induce a rotary windward meridian. Lockin requires a body-fixed asymmetry and a zero windward meridian rotation rate.[18] The latter can occur if the vehicle is trimmed or if it is untrimmed but precessing positively such that $\dot{\phi} = p - \omega_n$, which tends to zero as $p \to \omega_n$. By undamping the angle of attack with a negative yaw moment to induce negative precession, $\dot{\varphi} = p + \omega_n$, which approaches $2\omega_n$ at resonance crossing. The angle of attack required to induce negative precession, i.e., to untrim the angle of attack, depends on the magnitude of the trim asymmetry and the trim amplification or attenuation factor. It has been shown that the closed-loop angle-of-attack response to a trim asymmetry is attenuated by a factor that depends on the control system gain. Potentially, a small amount of undamping could induce a sufficient windward meridian rotation rate to prevent lockin.

Angle-of-attack control might be used instead of drag flaps as a drag control system. The control logic for such a system is shown in Fig. 10. The system could be used, for example, to decelerate a re-entry body for recovery.

V. Conclusions

The use of intentionally applied pitch and yaw moments to control the angle of attack of a spinning missile has been demonstrated. The angle of attack undamping due to a wind-fixed yaw moment is equal to the steady resonance amplification of the nonrolling trim angle of attack produced by an equal moment. The yaw moment undamping factor is relatively independent of the ratio of the roll rate to the natural pitch frequency, whereas the steady roll resonance trim amplification is a strong function of the roll rate ratio.

A root locus analysis of a closed-loop angle-of-attack control system with simple pitch rate feedback shows good stability behavior. The closed-loop angle-of-attack response to a body-fixed trim asymmetry shows, in general, an attenuation in trim angle of attack below the open-loop-steady-resonance value depending on the control system gain.

Several methods have been proposed for mechanizing an angle-of-attack control system. The essential feature for generating wind-fixed pitch and yaw moments is a rotating pendulum mass that is used directly to either rotate a trim generator at the windward meridian rotation frequency or to regulate the rotation frequency of a motor-driven trim generator. A new type of sensor system has been proposed that permits direct measurement of total angle of attack, pitch and yaw rates, and normal acceleration in a wind-referenced Euler angle coordinate system.

A simple passive angle-of-attack damper consists of a damped pendulum suspended aft of the missile center of gravity to permit rotation about the missile roll axis. The pendulum generates a yaw moment that damps the angle of attack for subcritical roll rates, undamps positive mode precession, and damps negative precession for supercritical roll rates.

A significant characteristic of yaw moment undamping is the rapid change in the precession rate of the lift vector from

the trimmed to the untrimmed condition. During rolling trimmed flight, the lift vector precesses at a rate approximately equal to the roll rate. As the angle of attack undamps, the precession rate rapidly approaches the pitch frequency. The windward meridian rotation rate also increases rapidly from near zero (lunar motion) to a relatively large value depending on the roll rate. This latter feature might be used advantageously to prevent resonance lockin by intentionally undamping the angle of attack in the proper mode just prior to resonance crossing.

References

[1] Boltz, R. E., "Dynamic Stability of a Missile in Rolling Flight," *Journal of the Aeronautical Sciences,* Vol. 19, June 1952, pp. 395-403.

[2] Murphy, C. H., "Effect of Roll on Dynamic Instability of Symmetric Missiles," *Journal of the Aeronautical Sciences,* Vol. 21, Sept. 1954, pp. 643-644.

[3] Nicolaides, J. D., "Two Non-Linear Problems in the Flight Dynamics of Modern Ballistic Missiles," Rept. 59-17, Jan. 1959, Institute of Aerospace Sciences, New York.

[4] Platou, A.S., "The Magnus Force on a Finned Body," BRL 1193, March 1963, Ballistic Research Labs., Aberdeen Proving Ground, Md.

[5] Benton, E. R., "Supersonic Magnus Effects on a Finned Missile," *AIAA Journal,* Vol. 2, Jan. 1964, pp. 153-155.

[6] Platou, A. A., "Magnus Characteristics of Finned and Non-Finned Projectiles," *AIAA Journal,* Vol. 3, Jan. 1965, pp. 83-90.

[7] Curry, W. H., and Reed, J. F., "Measurement of Magnus Effects on a Sounding Rocket Model in a Supersonic Wind Tunnel," AIAA Paper 65-754, Los Angeles, Calif., 1966.

[8] Uselton, J. C., and Carman, J. B., "A Study of the Magnus Effects on a Sounding Rocket at Supersonic Speeds," AIAA Paper 70-207, New York, N.Y., 1970.

[9] Waterfall, A. P., "Effect of Ablation on the Dynamics of Spinning Re-Entry Vehicles," *Journal of Spacecraft and Rockets,* Vol. 6, Sept. 1969, pp. 1038-1043.

[10] Platus, D. H., "Dynamic Instability of Finned Missiles Caused by Unbalanced Fin Forces," *AIAA Journal,* Vol. 9, March 1971, pp. 378-381.

[11] Chrusciel, G. T., "Analysis of R/V Behavior During Boundary-Layer Transition," AIAA Paper 74-109, Washington, D.C., 1974.

[12] Tolosko, R. J., "Amplification Due to Body Trim Plane Rotation," AIAA Paper 71-48, New York, 1971.

[13] Platus, D. H., "Angle of Attack Convergence and Windward-Meridian Rotation Rate of Rolling Re-Entry Vehicles," *AIAA Journal,* Vol. 7, Dec. 1969, pp. 2324-2330.

[14] Platus, D. H., "Reply by Author to C. H. Murphy," *AIAA Journal,* Vol. 8, July 1970, pp. 1374-1375.

[15] Nicolaides, J. D., "On the Free Flight Motion of Missiles Having Slight Configurational Asymmetries," BRL 858, AD 26405, June 1953, Ballistic Research Labs., Aberdeen Proving Ground, Md.

[16] Pettus, J. J., "Persistent Re-Entry Vehicle Roll Resonance," AIAA Paper 66-49, New York, 1966.

[17] Hopper, F. W., "Active Precession Control for Spin Stabilized Space Vehicles," AIAA Paper 71-952, Hempstead, New York, N.Y., 1971.

[18] Platus, D. H., "A Note on Re-Entry Vehicle Roll Resonance," *AIAA Journal,* Vol. 5, July 1967, pp. 1348-1350.